A continuum theory of amorphous solids undergoing large deformations, with application to polymeric glasses

Lallit Anand
Department of Mechanical Engineering
Massachusetts Institute of Technology
Cambridge, MA 02139, USA

Abstract— **This paper summarizes a recently developed continuum theory for the elastic-viscoplastic deformation of amorphous solids such as polymeric and metallic glasses. Introducing an internal-state variable that represents the local free-volume associated with certain metastable states, we are able to capture the highly non-linear stress-strain behavior that precedes the yield-peak and gives rise to post-yield strain-softening. Our theory explicitly accounts for the dependence of the Helmholtz free energy on the plastic deformation in a thermodynamically consistent manner. This dependence leads directly to a backstress in the underlying flow rule, and allows us to model the rapid strain-hardening response after the initial yield-drop in monotonic deformations, as well as the Bauschinger-type reverse-yielding phenomena typically observed in amorphous polymeric solids upon unloading after large plastic deformations. We have implemented a special set of constitutive equations resulting from the general theory in a finite-element computer program. Using this finite-element program, we apply the specialized equations to model the large-deformation response of the amorphous polymeric solid polycarbonate, at ambient temperature and pressure. We show numerical results to some representative problems, and compare them against corresponding results from physical experiments.**

Keywords— **A. Amorphous solids. B. Polymeric and metallic glasses. C. Plasticity**

I. Introduction

UNDER certain conditions many solids appear in a disordered form; such solids are referred to as *amorphous* or *glassy*. Important examples of amorphous solids are polymeric (molecular) glasses and metallic (atomic) glasses. While there are important differences in the microstructural mechanisms leading to plastic or inelastic deformations of polymeric and metallic amorphous solids, it is possible to develop a reasonably general constitutive framework for the inelastic deformation of such amorphous solids at the macroscopic level.[1] The purpose of this paper is to summarize a recently developed macroscopic theory for the elastic-viscoplastic deformation of an amorphous solid under isothermal conditions below its *glass transition temperature* (Anand and Gurtin [6]).

A significant advance in modeling the plastic deformation of amorphous polymers has been made by Parks, Argon, Boyce, Arruda, and their co-workers (e.g. [7], [8]). Our theory is based on physical ideas contained in these models, and, following these authors, we also utilize the Kröner-Lee decomposition, $\mathbf{F} = \mathbf{F}^e \mathbf{F}^p$, of the deformation gradient $\mathbf{F}$ into elastic and plastic parts, $\mathbf{F}^e$ and $\mathbf{F}^p$ ([9], [10]). An important feature of our theory is the assumption that the (Helmholtz) free energy depends on $\mathbf{F}^p$, an assumption that leads directly to a *backstress* in the underlying flow rule. Further, a key feature controlling the *initial* plastic deformation of amorphous materials is known to be the evolution of the local free-volume associated with certain metastable states, and it is commonly believed that for glassy polymers the evolution of this free-volume is the major reason for the highly non-linear stress-strain behavior that precedes the yield-peak and gives rise to post-yield strain-softening. Metallic glasses also show a "yield-drop" specially at high temperatures (e.g. [11]) In our theory, we represent this local free-volume by an internal-state variable η.[2]

The plan of this paper is as follows. In Section II we summarize a set of specialized constitutive equations that should be useful in applications[3] In Section III, we apply the specialized equations to model the large-deformation response of the amorphous polymeric solid, polycarbonate, at ambient temperature and pressure. Finally, Section IV contains concluding remarks.

II. Constitutive model

In terms of the variables

---

[1]We use the words plastic and inelastic interchangeably, and emphasize that the micro-mechanisms leading to such deformations in amorphous solids are not related to dislocation-based micro-mechanisms that characterize the plastic deformation of crystalline metals. Cf. [1] for a review on the micromechanisms of plastic deformation of amorphous solids. For a review of the physics of glassy polymers see [2] and [3]. For some recent reviews on aspects of bulk metallic glasses see [4] and [5].

[2]The material itself is presumed to be plastically incompressible. We believe that because of the disparate difference between the scale of the macroscopic deformation and the scale of the local free-volume, the latter is better represented by an internal-state variable rather than by $J^p = \det \mathbf{F}^p$. In fact, in a previous version of this work we used J^p rather than η; the final equations were far more complicated, but order-of-magnitude calculations as well as numerical calculations for polycarbonate lead us to believe that the predictions of the two theories would differ little.

[3]For detailed derivations the reader is referred to Anand and Gurtin [6].

$$\mathbf{T}, \quad \mathbf{T} = \mathbf{T}^{\top}, \qquad \text{Cauchy stress,}$$

$$\mathbf{F}, \quad \det\mathbf{F} > 0, \qquad \text{deformation gradient,}$$

$$\mathbf{F}^p, \quad \det\mathbf{F}^p = 1, \quad \text{plastic deformation gradient,}$$

$$s, \quad s > 0, \qquad\qquad \text{isotropic resistance to plastic flow,}$$

$$\eta, \qquad\qquad\qquad \text{free volume,}$$

and the definitions

$$\mathbf{F}^e = \mathbf{F}\mathbf{F}^{p-1}, \ \det\mathbf{F}^e > 0, \quad \text{elastic deformation gradient,}$$

$$\mathbf{C}^e = \mathbf{F}^{e\top}\mathbf{F}^e,$$

$$\mathbf{E}^e = \tfrac{1}{2}(\mathbf{C}^e - \mathbf{1}), \qquad \text{elastic strain,}$$

$$\mathbf{T}^e = \mathbf{R}^{e\top}\mathbf{T}\mathbf{R}^e, \qquad \text{elastic stress,}$$

$$\pi = -\tfrac{1}{3}\operatorname{tr}\mathbf{T}, \qquad\qquad \text{mean normal pressure,}$$

$$\mathbf{T}_0^e = \mathbf{T}^e + \pi\mathbf{1}, \qquad\qquad \text{deviatoric stress,}$$

$$\mathbf{B}^p = \mathbf{F}^p\mathbf{F}^{p\top},$$

$$\mathbf{B}_0^p = \mathbf{B}^p - \tfrac{1}{3}(\operatorname{tr}\mathbf{B}^p)\mathbf{1}, \qquad \text{deviatoric part of } \mathbf{B}^p,$$

$$\lambda^p = \tfrac{1}{\sqrt{3}}\sqrt{\operatorname{tr}\mathbf{B}^p}, \qquad\qquad \text{effective plastic stretch,}$$

we summarize below a set of constitutive equations that should be useful in applications:

1. **Free Energy**:

$$\psi = \psi^e + \psi^p, \tag{1}$$
$$\psi^e = G|\mathbf{E}_0^e|^2 + \tfrac{1}{2}K|\operatorname{tr}\mathbf{E}^e|^2, \tag{2}$$
$$\psi^p = \Psi(\lambda^p) \geq 0, \qquad \Psi(1) = 0. \tag{3}$$

Here G and K are the elastic shear and bulk moduli, respectively.

2. **Equation for the stress**:

$$\mathbf{T}^e = 2G\mathbf{E}_0^e + K(\operatorname{tr}\mathbf{E}^e)\mathbf{1}. \tag{4}$$

3. **Flow rule**:
The evolution equation for $\mathbf{F}^p$ is

$$\dot{\mathbf{F}}^p = \mathbf{D}^p\mathbf{F}^p, \qquad \mathbf{F}^p(\mathbf{X}, 0) = \mathbf{1}, \tag{5}$$

with $\mathbf{D}^p$ given by the flow rule

$$\mathbf{D}^p = \nu^p\left(\frac{\mathbf{T}_0^e - \mu\mathbf{B}_0^p}{2\bar{\tau}}\right), \qquad \nu^p = \nu_0\left(\frac{\bar{\tau}}{s + \alpha\pi}\right)^{\frac{1}{m}}, \tag{6}$$

where

$$\bar{\tau} = \frac{1}{\sqrt{2}}\,|\mathbf{T}_0^e - \mu\mathbf{B}_0^p|, \qquad \nu^p = \sqrt{2}\,|\mathbf{D}^p|, \tag{7}$$

are an *equivalent shear stress* and *an equivalent plastic shear strain rate*. Here, $\nu_0 > 0$ is a *reference plastic shear strain rate*, and $0 < m \leq 1$ is a *strain rate sensitivity parameter*. The limit $m \to 0$ corresponds to a rate-independent response, while the limit $m \to 1$ to a linear viscous response.[4] The parameter α represents a

[4]More elaborate form of rate sensitivity may be introduced, however, a simple power-law form makes the structure of theory more transparent.

pressure sensitivity of plastic flow, where we require that $(s + \alpha\pi) > 0$. Also,

$$\mu = \frac{1}{3\lambda^p}\,\frac{\partial\Psi}{\partial\lambda^p} > 0, \tag{8}$$

represents a *back stress modulus*.

4. **Evolution equations for the internal variables s and η**:

$$\left.\begin{aligned}
\dot{s} &= h(\pi, \lambda^p, \eta, s, \nu^p), \qquad s(\mathbf{X}, 0) = s_0, \\
\dot{\eta} &= g(\pi, \lambda^p, \eta, s, \nu^p), \qquad \eta(\mathbf{X}, 0) = 0,
\end{aligned}\right\} \tag{9}$$

with s_0 a constitutive modulus that represents the initial resistance to flow. Here h, may take on positive (hardening) and negative (softening) values. Also, as is tacit from $(9)_2$, the free volume is measured from the value $\eta = 0$ in the virgin state of the material, and thus η at any other time represents a change in the free-volume from the initial state.[5]

To complete the constitutive model for a particular amorphous material the constitutive parameter/functions that need to be specified are

$$\{G, K, \Psi, h, g, s_0\}.$$

III. APPLICATION TO AN AMORPHOUS POLYMERIC SOLID

In this section we further specialize our constitutive model and apply it to describe the deformation response of the technologically important amorphous polymeric solid, polycarbonate, at atmospheric pressure and room temperature.[6]

In amorphous polymeric materials the major part of ψ^p arises from an "entropic" contribution. Motivated by statistical mechanics models of rubber elasticity (cf., [12], [13], [14]) we consider two specific forms:

1. For small to moderate values of λ^p, we consider the simple *neo-Hookean* form

$$\psi^p = \mu\,\frac{3}{2}\left\{(\lambda^p)^2 - 1\right\}, \tag{10}$$

with μ a *constant* equal to the backstress modulus (8).

2. For larger values of λ^p, we consider the *Langevin-inverse* form

$$\psi^p = \mu_R\,\lambda_L^2\left[\left(\frac{\lambda^p}{\lambda_L}\right)x + \ln\left(\frac{x}{\sinh x}\right)\right. \tag{11}$$

$$\left. -\left(\frac{1}{\lambda_L}\right)y - \ln\left(\frac{y}{\sinh y}\right)\right], \tag{12}$$

$$x = \mathcal{L}^{-1}\left(\frac{\lambda^p}{\lambda_L}\right), \qquad y = \mathcal{L}^{-1}\left(\frac{1}{\lambda_L}\right), \tag{13}$$

where $\mathcal{L}^{-1}$ is the inverse[7] of the Langevin function $\mathcal{L}(\cdots) = \coth(\cdots) - (\cdots)^{-1}$. This functional form for ψ^p involves

[5]More generally, one would use an initial value η_0, but the small 'free volume' in amorphous polymers and glasses is, at present, hard to determine experimentally.

[6]The glass transition temperature for polycarbonate is $\approx 145°$ C.

[7]To evaluate $x = \mathcal{L}^{-1}(y)$ for a given y in the range $0 < y < 1$, we numerically solve the non-linear equation $f(x) = \mathcal{L}(x) - y = 0$ for x.

two material parameters: μ_R, called the *rubbery modulus*, and λ_L called the *network locking stretch*. In this case, from (8), the backstress modulus is

$$\mu = \mu_R \left(\frac{\lambda_L}{3\lambda^p}\right) \mathcal{L}^{-1}\left(\frac{\lambda^p}{\lambda_L}\right). \tag{14}$$

The modulus $\mu \to \infty$ as $\lambda^p \to \lambda_L$, since $\mathcal{L}^{-1}(z) \to \infty$ as $z \to 1$.

Graphs of ψ^p versus λ^p for representative values[8] of material parameters for the neo-Hookean energy ($\mu = 16.95\,\mathrm{MPa}$), and for the form involving the inverse Langevin function ($\mu_R = 11\,\mathrm{MPa}, \lambda_L = 1.45$) are shown in Fig. 1a. The corresponding graphs for the backstress modulus μ are shown in Fig. 1b.

We consider the evolution equations (9) in the special coupled rate-independent form[9]

$$\left.\begin{aligned}
\dot{s} &= h_0\left(1 - \frac{s}{\tilde{s}(\eta)}\right)\nu^p, \\
\dot{\eta} &= g_0\left(\frac{s}{s_{\mathrm{cv}}} - 1\right)\nu^p,
\end{aligned}\right\} \tag{15}$$

with

$$\tilde{s}(\eta) = s_{\mathrm{cv}}[1 + b(\eta_{\mathrm{cv}} - \eta)], \tag{16}$$

where $\{h_0, g_0, s_{\mathrm{cv}}, b, \eta_{\mathrm{cv}}\}$ are additional material parameters. Here $\tilde{s} = \tilde{s}(\eta)$ is a saturation value of s: $\dot{s}$ is positive for $s < \tilde{s}$ and negative for $s > \tilde{s}$. By definition ν^p is non-negative. Assuming that $\nu^p > 0$, we may by a change in time scale transform (15) into a pair of ODEs. This system has a single equilibrium point $(s_{\mathrm{cv}}, \eta_{\mathrm{cv}})$ in the (s, η)-plane, and it is globally stable. Thus all solutions satisfy

$$s \to s_{\mathrm{cv}} \quad \text{and} \quad \eta \to \eta_{\mathrm{cv}} \quad \text{as} \quad t \to \infty.$$

We restrict attention to the initial conditions $s = s_0$ and $\eta = 0$, with

$$s_0 \leq s \leq s_{\mathrm{cv}}(1 + b\eta_{\mathrm{cv}}).$$

Then a study of the phase portrait shows that η increases monotonically to its equilibrium value η_{cv}, while s increases monotonically to a peak and then decreases monotonically to its equilibrium value s_{cv}, thus capturing the observed yield-peak in the flow resistance.

We have implemented our constitutive model in the finite-element computer program ABAQUS/Explicit [15] by writing a user material subroutine. Using this finite-element program, we next present results to some representative problems.

A stress-strain curve obtained from a monotonic simple compression experiment[10] conducted at a constant logarithmic strain rate of -0.001/s is shown in Fig. 2; absolute

values of stress and strain are plotted. After an initial approximately linear region, the stress-strain curve becomes markedly nonlinear prior to reaching a peak in the stress; the material then strain-softens to a quasi-plateau before beginning a broad region of rapid strain hardening.

We discuss below the results of our efforts at *estimation* of the material parameters for our constitutive model.[11] Recall that the material parameters that need to be determined are

1. The elastic shear and bulk moduli (G, K) in the elastic part of the free energy.
2. The parameter μ in the neo-Hookean form, or the parameters (μ_R, λ_L) in the inverse Langevin form of the plastic free energy.
3. The parameters $\{\nu_0, m, \alpha, h_0, g_0, s_{cv}, b, \eta_{cv}, s_0\}$ in the flow rule and the evolution equations for (s, η).

The values of (G, K) are determined by measuring the Young's modulus and Poisson's ratio of the material in a compression experiment and using standard conversion relations of isotropic elasticity to obtain the elastic shear and bulk moduli. The parameters $\{\nu_0, m\}$ are estimated by conducting a strain rate jump experiment in simple compression, and the pressure sensitivity parameter α is estimated from compression experiments under superposed hydrostatic pressure reported in the literature. The parameters $\{h_0, g_0, s_{cv}, b, \eta_{cv}, s_0\}$ and (μ_R, λ_L) may be estimated by fitting a stress-strain curve in compression to large strains. Once (μ_R, λ_L) are estimated so as to fit the data for large strains, then the value of μ in the neo-Hookean form of ψ^p is easily obtained from (14) as the limit at $\lambda^p = 1$.

Using a value of $\alpha = 0.08$ from the data reported by [16], a value of $\nu_0 = 0.0017\,\mathrm{s}^{-1}$ and a strain rate-sensitivity parameter $m = 0.011$ obtained from a strain rate jump experiment, the parameters $\{G, K, \mu_R, \lambda_L, h_0, g_0, s_{cv}, b, \eta_{cv}, s_0\}$ were estimated by fitting the stress-strain curve for polycarbonate in simple compression, Fig. 2. The fit was performed by judiciously adjusting the values of these parameters in finite element simulations of a simple compression experiment (assuming homogeneous deformation) using a single ABAQUS/C3D8R element. After a few attempts, a reasonable fit was obtained, and this is shown in Fig. 2a. The list of parameters obtained using this heuristic calibration procedure are:[12]

---

[8]These numbers are based on our estimates (to be discussed shortly) for polycarbonate.

[9]We expect that $\tilde{s}$ (and perhaps h_0 and g_0) may, in general, depend on ν^p, but currently there is insufficient experimental evidence to warrant such a refinement.

[10]All experiments reported in this paper were performed by Dr. B. P. Gearing as part of his doctoral research at MIT. As is well known, the mechanical response of amorphous thermoplastics is very sensi-

tive to prior thermo-mechanical processing history. The experiments were conducted on polycarbonate specimens which were annealed at the glass transition temperature of this material, $145°\mathrm{C}$, for 2 hours, and then furnace-cooled to room temperature in approximately 15 hours. The experiments reported here were conducted under isothermal conditions at room temperature.

[11]We have not attempted to carry out a comprehensive experimental program to obtain precise numbers for polycarbonate. The purpose of this section is to emphasize only the qualitative features of the theory. We leave a more detailed comparison of theory against experiment for future work.

[12]This list, although not unique, seems adequate for illustrative purposes.

$$G = 0.857\text{GPa} \quad K = 2.24\text{GPa}$$
$$\mu_R = 11.0\text{MPa} \quad \lambda_L = 1.45$$
$$\nu_o = 0.0017\text{s}^{-1} \quad m = 0.011$$
$$\alpha = 0.08$$
$$h_0 = 2.75\text{GPa} \quad s_{cv} = 24.0\text{MPa}$$
$$b = 825 \quad \eta_{cv} = 0.001$$
$$g_0 = 6.0 \cdot 10^{-3} \quad s_0 = 20.0\text{MPa}$$

Fig. 2b shows a comparison of the stress-strain response calculated using the inverse Langevin form for ψ^p and the list of material parameters above, against the stress-strain response calculated using the neo-Hookean form for ψ^p with the same material parameters, except that the pair of constants (μ_R, λ_L) are replaced by the single constant $\mu = 16.95\,\text{MPa}$. This comparison shows that the simple neo-Hookean form for ψ^p may be adequate for applications involving logarithmic strains less than $\approx 35\%$. In the remaining part of our discussion we shall concentrate on the predictions of the model using the inverse Langevin form of ψ^p.

A representative stress-strain curve obtained from a simple compression experiment conducted to a strain level of ≈ -0.9, and then unloaded to zero stress is shown in Fig. 3. The experiment clearly exhibits reverse yielding upon unloading due to the development of a backstress. A corresponding numerical calculation which exhibits the same response is also shown in Fig. 3. The numerical simulation was carried out using the material parameters determined by fitting the *monotonic compression experiment*, as discussed above; the unloading part of the stress-strain curve was not used to adjust the material parameters. The correspondence between the predicted unloading response from the model and the actual experiment is very encouraging.

Finally, Fig. 4a shows a representative experimentally-measured load-displacement curve in a tension experiment on a specimen with a cylindrical gauge section. At the peak load a pronounced neck forms in the gauge section, the load subsequently decreases to an approximate plateau value, and the neck propagates along the gauge section. To numerically model this experiment, one half of a specimen was meshed with 390 ABAQUS/CAX4R axisymmetric elements. As before, the constitutive parameters used in the simulation are those obtained from the fitting exercise for the compression experiment. The calculated load-displacement response is also shown in Fig. 4a. Deformed geometries are shown in Fig. 4 b,c at the two displacement levels which have been marked in Fig. 4a. The deformation is homogeneous until the peak load. Subsequent to the peak load, at location 1, a localized neck has formed at the center of the gauge section, and by stage 2 the neck has propagated along the gauge section, as was observed in the corresponding experiment.

IV. Concluding remarks

We have shown an application of our theory to an amorphous polymeric solid in the previous section. Here the explicit dependence of the Helmholtz free energy on $\mathbf{F}^p$, led us directly to a resistance to plastic flow as represented by the backstress $(\mu \mathbf{B}_0^p)$. For amorphous metallic solids we expect that the dependence of the free energy on $\mathbf{F}^p$ should be considerably smaller than that in amorphous polymers,[13] and in this case we expect that our constitutive model should also be applicable, provided the backstress in the model is neglected.[14]

The current generation of bulk metallic glasses are believed to have many potential applications resulting from their unique properties: superior strength ($\approx 2\,\text{GPa}$), and high yield strain ($\approx 2\%$); thus the elastic strain energy that can be stored in these materials is extremely high (e.g., [4], [5]). However, when a metallic glass is deformed at ambient temperatures the plastic deformation is inhomogeneous, and is characterized by the formation of intense localized shear bands;[15] fracture typically occurs after very small inelastic strain in tension, and an inelastic strain of only a few percent in compression. In contrast, these materials exhibit a high strain-rate sensitivity (large value of m), and large inelastic strains at temperatures greater than approximately 70% of the glass transition temperature of the material. This opens the possibility of using conventional metal forming technologies to manufacture structural components from this relatively new class of materials. Thus there is growing interest in studying the large deformation response of bulk metallic glasses in this high temperature range (e.g. [19]). We believe that our constitutive model, when suitably calibrated, might be useful for such applications.

References

[1] A. S. Argon, *Materials Science and Technology*, 1993, **6**, 461.
[2] R. N. Haward, *The Physics of Glassy Polymers*, 1973, Wiley.
[3] R. N. Haward, and R. J. Young, Editors, *The Physics of Glassy Polymers. Second Edition*, 1997, Chapman and Hall.
[4] W. L. Johnson, *MRS Bulletin*, 1999, **24(10)**, 7249.
[5] A. Inoue, *Acta Materialia*, 2000, **48**, 279.
[6] L. Anand, and M. E. Gurtin, *International Journal of Solids and Structures*, 2002, in press.
[7] M. C. Boyce, D. M. Parks, and A. S. Argon, *Mechanics of Materials"*, 1998, **7**, 15.
[8] E. M. Arruda and Boyce, M. C., *International Journal of Plasticity*, 1998, **9**, 697.

[13] The two-dimensional molecular dynamic simulations of the deformation of an atomic glass of [17] do show the development of a Bauschinger effect, their Figure 8. However, we have not found a report of the Bauschinger effect in atomic glasses in physical experiments on these materials at the macroscopic level.

[14] Indeed, if the material is further idealized as plastically pressure-insensitive and one drops the internal variable η, then one recovers an isotropic elastic-viscoplastic constitutive model similar in form to models which are widely used for isotropic polycrystalline metallic materials (e.g.,[18])

[15] Which we expect our strain-softening model to capture.

[9] E. Kroner, *Archive for Rational Mechanics and Analysis*, 1960, **4**, 273.

[10] E. H. Lee, *ASME Journal of Applied Mechanics*, 1969, **36**, 1.

[11] P. D. Hey, J. Sietsma, and A. Vandenbeukel, *Acta Materialia*, 1998, **46**, 5873.

[12] L. R. G. Treloar, *The Physics of Rubber Elasticity*, 1975, Oxford.

[13] E. M. Arruda, and M.C. Boyce, *Journal of the Mechanics and Physics of Solids*, 1993, **41**, 389.

[14] L. Anand, *Computational Mechanics*, 1996, **18**, 339.

[15] *ABAQUS/Explicit Reference Manuals*, 2002, Providence, R.I.

[16] W. A. Spitzig, and O. Richmond, *Polymer Engineering and Science*, 1979, **19**, 1129.

[17] D. Deng, A. S. Argon, and S. Yip, *Philosophical Transactions of the Royal Society A*, 1989, bf 329, 613.

[18] G. Weber, and L. Anand, *Computer Methods In Applied Mechanics and Engineering*, 1990, **79**, 173.

[19] T. G. Nieh, J. Wadsworth, C. T. Liu, T. Ohkubo, and Y. Hirotsu, *Acta Materialia*, 2001, **49**, 2887.
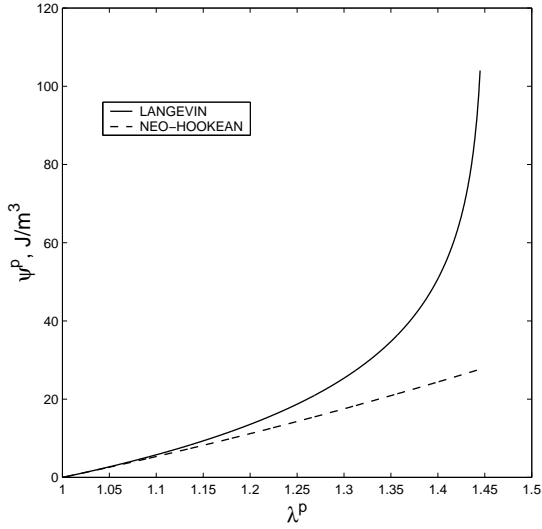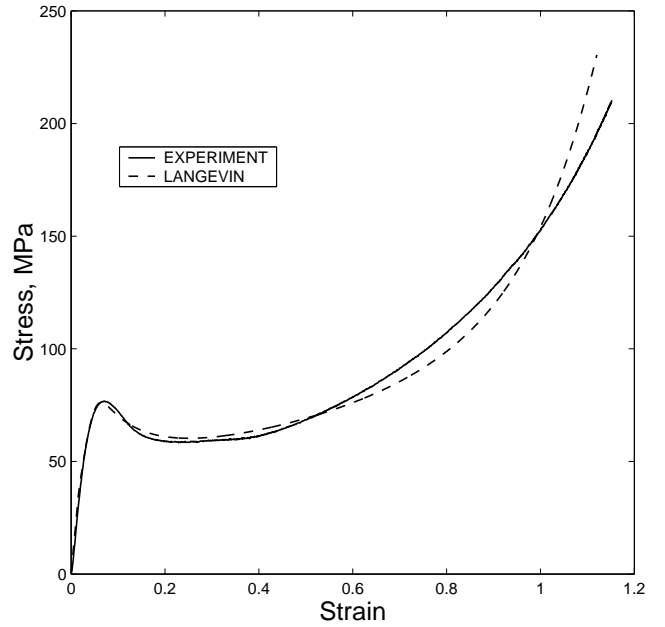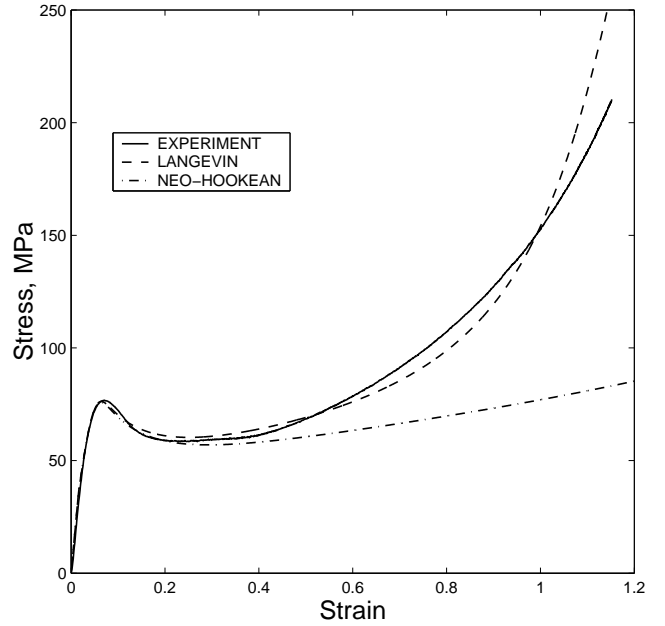
(a)
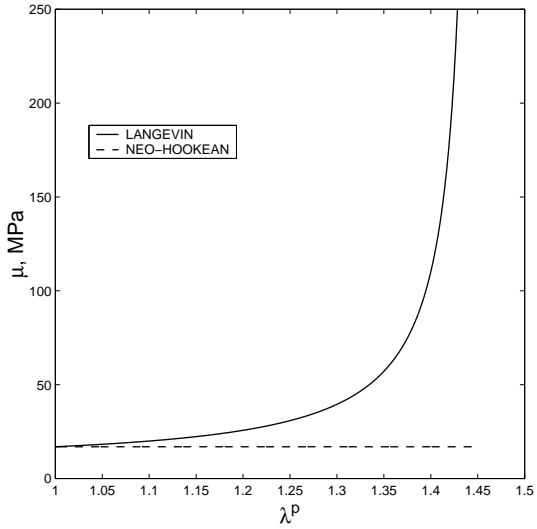
(b)

Fig. 1.   (a) Comparison of the Langevin inverse and neo-Hookean forms of the plastic free energy ψ^p. (b) Comparison of the corresponding forms for the backstress modulus μ.

(a)

(b)

Fig. 2.   (a) Stress-strain response of polycarbonate in simple compression, together with a fit of the constitutive model using the Langevin form for ψ^p. (b) Comparison of the stress-strain responses calculated using the Langevin form and the neo-Hookean form for ψ^p.
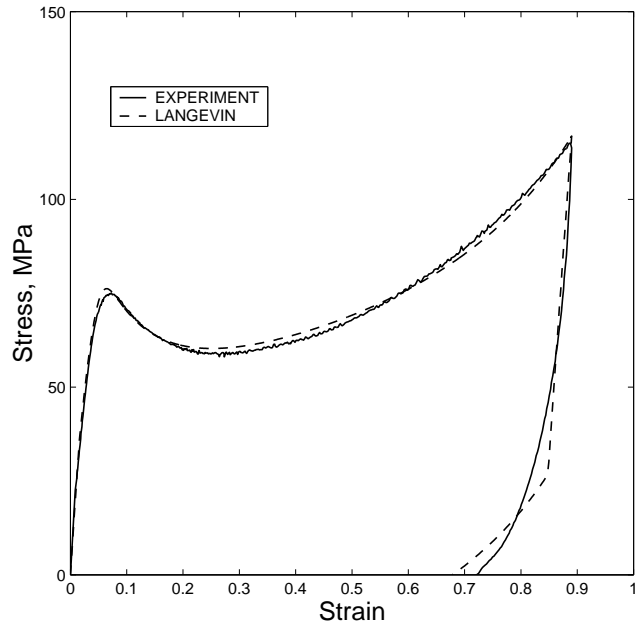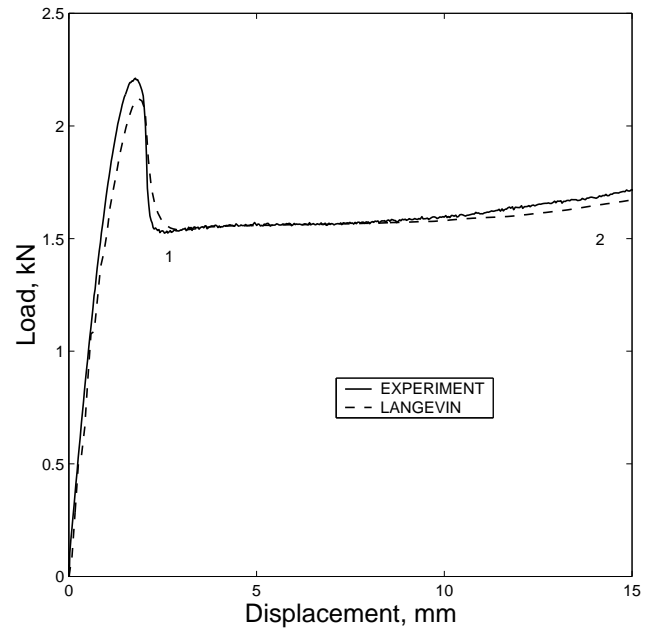
(a)

(b)

(c)

Fig. 4. (a) Experimental and numerical load-displacement curves in tension; two displacement levels of interest are marked. (b) Deformed geometry at displacement level 1 showing the beginnings of neck formation; (c) at displacement level 2 showing that the neck has propagated along the gauge section of the specimen.

Fig. 3. Stress-strain response of polycarbonate in simple compression showing reverse yielding upon unloading due to the development of back stress. The calculated response shows the same phenomenon.